BULLETIN
OF THE
CHEMICAL SOCIETY OF JAPAN

http://www.csj.jp/journals/bcsj/

Volume 82, Number 6, June 2009

Award Accounts

The Chemical Society of Japan Award for Creative Work for 2006

Phthalocyanine, Porphyrin, Cyclodextrin, and Polymer Systems Suitable for Studying by Circular Dichroism, Magnetic Circular Dichroism, and/or Electrochemistry

N. Kobayashi* and T. Fukuda

Bull. Chem. Soc. Jpn. **2009**, *82*, 631–663

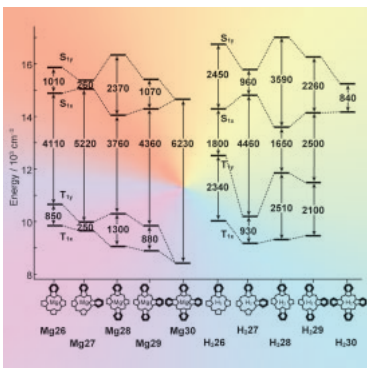

The author's recent electronic absorption, CD, and MCD studies on porphyrins, phthalocyanines, optically active polymers, and cyclodextrin systems are briefly reviewed. Emphasis is placed on the elucidation of molecular structure–spectroscopic property relationships in spectroscopically representative systems.

BCSJ Award Article

Effect of Hydration on the Very Slow Droplet–Lamellar Transition in Dioleylsulfosuccinate/Decane/Water System: A Small Angle X-ray Scattering Study

S. K. Ghosh, N. Ichiyanagi, H. Okabayashi,* A. Yoshino, T. Takeda, and C. J. O'Connor

Bull. Chem. Soc. Jpn. **2009**, *82*, 664–674

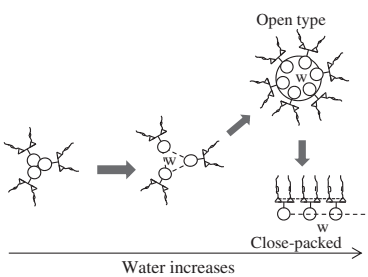

In the sodium dioleylsulfosuccinate (SDOleS)–decane–water system with various molar ratios of water and SDOleS ($X = [H_2O]/[SDOleS]$), the droplet lamellar transition occurs very slowly and spontaneously depending upon X.

Aromaticity and Conjugation in Sapphyrin and Orangarin

J. Aihara* and M. Makino

Bull. Chem. Soc. Jpn. **2009**, *82*, 675–682

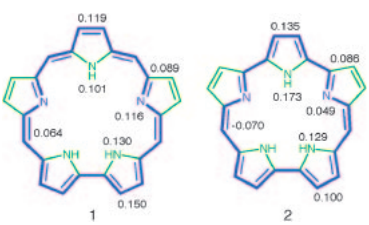

BREs in units of $|\beta|$ and main macrocyclic conjugation pathways.

Aromaticity and ring-current diamagnetism in two expanded porphyrins, sapphyrin (**1**) and orangarin (**2**), were analyzed theoretically. Main macrocyclic conjugation pathways in these π-systems were predicted consistently from the bond resonance energies (BREs) and the π-current density maps.

Configuration of Adsorbed Phases and Their Evolution to Absorbent States in the CH_4–O_2 Catalytic Reaction

J. Cortés* and E. Valencia

Bull. Chem. Soc. Jpn. **2009**, *82*, 683–688

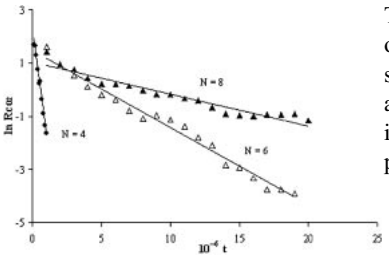

Through kinetic Monte Carlo simulations of the catalytic oxidation of methane, it is shown that the temporal evolution of the adsorbed phase to absorbent states is interpreted by an exponential decay of production ($R_i \approx e^{-kt}$).

Kinetic Study of Singlet-Oxygen Quenching by Caffeic Acid and Related Phenols

K. Ohara,* Y. Ichimura, and S. Nagaoka

Bull. Chem. Soc. Jpn. **2009**, *82*, 689–691

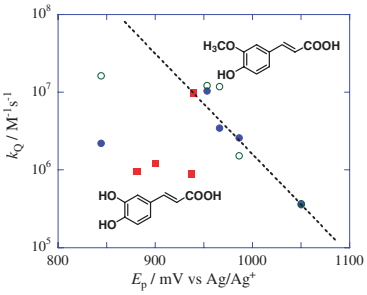

The second-order rate constants (k_Q) of singlet-oxygen quenching by caffeic acid and related phenols were measured in ethanol and toluene. These phenols deactivate singlet-oxygen by physical quenching at $k_Q = 10^6$–10^7 M^{-1} s^{-1} through a charge-transfer transition state.

Purity Effects on the Charge-Transport Properties in One-Dimensional $TPP[Co^{III}(Pc)(CN)_2]_2$ (TPP = Tetraphenylphosphonium and Pc = Phthalocyaninato) Conductors

S. Yamashita, T. Naito, and T. Inabe*

Bull. Chem. Soc. Jpn. **2009**, *82*, 692–694

Purity effects on the electrical resistivity in $TPP[Co(Pc)(CN)_2]_2$ with a one-dimensional metallic electronic system have been examined. No dependence on the impurity content has been observed, suggesting that the thermally activated behavior is dominated by charge disproportionation.

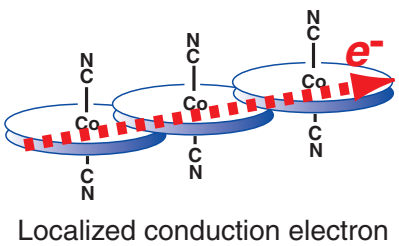

Selected Paper

Three-Dimensional Morphological Chirality Induction in Polythiophene Polymer Deposit Using a Magnetic Field

Y. Tanimoto,* A. Shinyama, and K. Omote

Bull. Chem. Soc. Jpn. **2009**, *82*, 695–697

In the presence of a 4-T vertical magnetic field, left-handedly and right-handedly twisted polymer deposits are obtained when prepared by anodic oxidation.

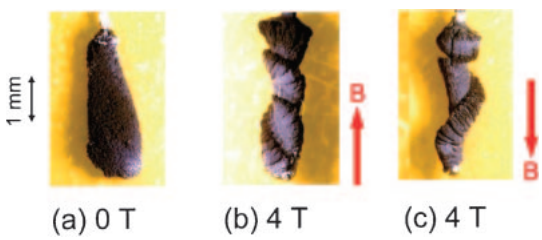

Chloride Complexation of Zr and Hf in HCl Investigated by Extended X-ray Absorption Fine Structure Spectroscopy: Toward Characterization of Chloride Complexation of Element 104, Rutherfordium (Rf)

H. Haba,* K. Akiyama, K. Tsukada, M. Asai, A. Toyoshima, T. Yaita, M. Hirata, K. Sueki, and Y. Nagame

Bull. Chem. Soc. Jpn. **2009**, *82*, 698–703

Chloride complexation of Zr and Hf in HCl is investigated by EXAFS spectroscopy to characterize chloro complexes of element 104, rutherfordium (Rf). Together with the anion-exchange results, it is suggested that Rf forms the same complexes as those with Zr and Hf, $[Rf(H_2O)_8]^{4+} \rightarrow [RfCl_6]^{2-}$, and that the affinity of Cl^- for these metal ions is in the order of Rf > Zr > Hf.

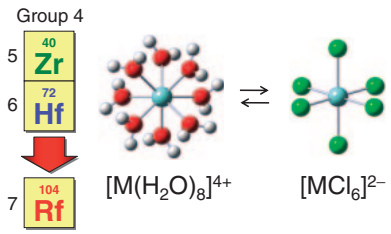

High-Resolution Solid-State NMR Studies of Natural Abundant ^{15}N Observed in Halogen-Bridged One-Dimensional Complexes, $[NiX(chxn)_2]X_2$ and $[Pd(chxn)_2]$-$[PdX_2(chxn)_2]Y_4$ (chxn = (1*R*,2*R*)-Diaminocyclohexane; Y = X (Halogen), NO_3, and ClO_4)

N. Kimura,* T. Shimizu, and R. Ikeda

Bull. Chem. Soc. Jpn. **2009**, *82*, 704–708

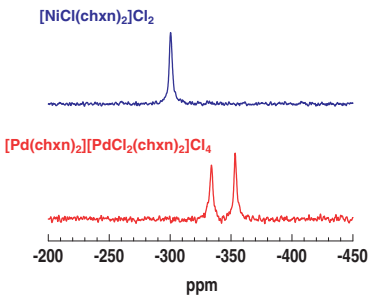

We performed solid-state ^{15}N NMR measurements of chxn ligands in halogen-bridged Pd and Ni complexes with a 1-D structure. Spectra obtained for ^{15}N bonded to Pd^{2+}, Pd^{4+}, and Ni^{3+} were clearly separated from each other.

^1H and ^{27}Al NMR Study of $Li[AlH_4]$ + Ti Compounds in Solution

S. Takeuchi, H. Senoh, S. Zhang, H. T. Takeshita, T. Kiyobayashi,* Q. Xu, and N. Kuriyama

Bull. Chem. Soc. Jpn. **2009**, *82*, 709–711

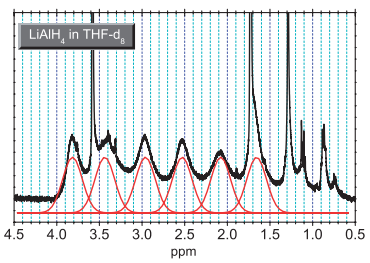

A broad sextet signal in the ^1H NMR spectrum of $Li[AlH_4]$ in THF-d_8, centering at 2.75 ppm with J/Hz = 176, was assigned to the signal from $[AlH_4]^-$. Also investigated were the reactions of $Li[AlH_4]$ with $TiCl_3$ or $Ti(OBu)_4$ in THF.

How Are Non-Bonded G···Z (Z = O, S, and Se) Distances at Benzene 1,2-, Naphthalene 1,8-, and Anthracene 1,8,9-Positions Controlled? An Approach to Causality in Weak Interactions

S. Hayashi and W. Nakanishi*

Bull. Chem. Soc. Jpn. **2009**, *82*, 712–722

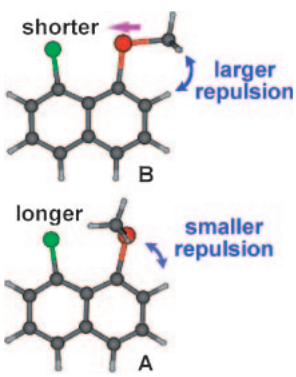

It is often difficult to demonstrate causality in weak interactions. Categories in weak interactions are sometimes quite different from those in strong interactions. Factors to control the non-bonded G···Z distances in 8-G-1-$RZC_{10}H_6$ are analyzed as a typical case, which is controlled not by the G···Z interaction but by the repulsive interaction between R and H at the 2-position.

Synthesis and Photochemical Characteristics of Amphiphilic Enediyne Dendrimers

N. Yoshimura, A. Momotake, Y. Shinohara, K. Takahashi, R. Nagahata, Y. Nishimura, and T. Arai*

Bull. Chem. Soc. Jpn. **2009**, *82*, 723–729

Amphiphilic enediyne-cored dendrimers were prepared as pure cis and trans isomers and the structure–photochemical property relationship is discussed.

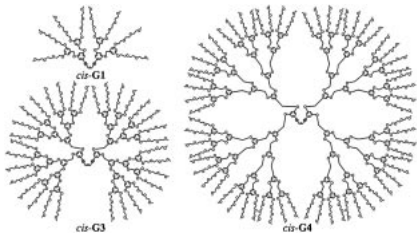

Synthesis and Structural Analysis of Triphenylmethane-Based Alkanecarboxamides and Their Assembly into Nanometer-Size Fibrous Objects

H. Houjou,* T. Koga, M. Akiizumi, I. Yoshikawa, and K. Araki

Bull. Chem. Soc. Jpn. **2009**, *82*, 730–736

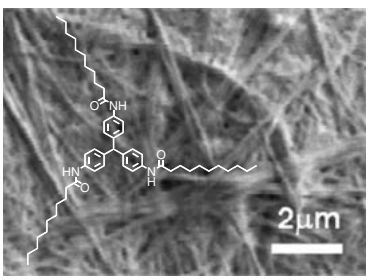

The molecular assembly of a series of C_3-symmetric trialkanecarboxamides was systematically investigated. The length of the alkyl chains considerably influenced the mode of crystal growth, which in turn caused a drastic change from microcrystals to fibrous objects with 100-nm thickness.

Photolysis of 1,2-Naphthoquinone in Oxygen-Doped Argon Matrix at Low Temperature

T. Itoh, J. Tatsugi,* and H. Tomioka*

Bull. Chem. Soc. Jpn. **2009**, *82*, 737–742

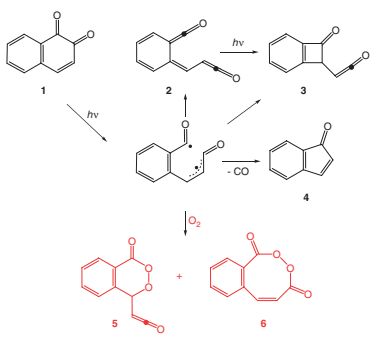

Photolysis of 1,2-naphthoquinone (**1**) in argon matrix gave bis(ketene) **2**, which isomerized to isomeric ketene **3** upon continued irradiation, along with a small amount of inden-1-one (**4**). When the irradiation was carried out in argon matrix doped with 20% oxygen, six- and eight-membered cyclic peroxide **5** and **6** presumably formed by trapping of initial diradical generated by α-cleavage of **1** upon photoexcitation by molecular oxygen were detected.

A Stable Electroactive Monolayer Composed of Soluble Single-Walled Carbon Nanotubes on ITO

Q. Wang and H. Moriyama*

Bull. Chem. Soc. Jpn. **2009**, *82*, 743–749

A monolayer composed of soluble single-walled carbon nanotubes on ITO was obtained, which showed stable electroactive behavior upon oxidation in acidic aqueous solutions after being endcapped by a conductive oligomer.